

# Geographical and seasonal distribution of tropical tropopause thin clouds and their relation to deep convection and water vapor viewed from satellite measurements

Chuntao Liu<sup>1</sup>

Received 4 May 2006; revised 8 November 2006; accepted 15 December 2006; published 3 May 2007.

[1] The climatologies of deep convection, thin clouds, and water vapor measurements from four independent satellites are compared in this study. Deep convection reaching the tropical tropopause layer (TTL) is indicated by the area of the Tropical Rainfall Measuring Mission (TRMM) precipitation radar (PR) 20 dBZ reflectivity reaching 14 km and the area of the TRMM visible and infrared scanner (VIRS) brightness temperature at 10.8  $\mu\text{m}$  ( $T_{B11}$ )  $< 210$  K. TTL clouds are identified by 17 years of Stratospheric Aerosol and Gas Experiment (SAGE) II measurements and by 1 year of Earth Observing System (EOS) Microwave Limb Sounder (MLS) ice water content in 2005. TTL water vapor is estimated from 2005 EOS MLS retrievals. Results suggest that TTL clouds are geographically and seasonally correlated with deep convection as inferred from the area of  $T_{B11} < 210$  K. Patterns of regional differences of seasonal variations of deep convection are also related to the regional differences of seasonal variations of TTL clouds. By grouping the Ice Cloud and Land Elevation Satellite/Geoscience Laser Altimeter System (ICESat/GLAS) layer cloud products, we find that there is a general spatial correlation between the largest, thickest TTL layer clouds with the highest optical depth and the regions with the most intense deep convection. MLS CO and water vapor at 146 hPa have similar geographical and seasonal variations as deep convection and TTL clouds. EOS MLS 100 hPa water vapor is low over the west Pacific Ocean at the same location and time as more TTL clouds are observed.

**Citation:** Liu, C. (2007), Geographical and seasonal distribution of tropical tropopause thin clouds and their relation to deep convection and water vapor viewed from satellite measurements, *J. Geophys. Res.*, 112, D09205, doi:10.1029/2006JD007479.

## 1. Introduction

[2] In recent years, there have been a number of studies of the water vapor budget in the tropical upper troposphere and lower stratosphere, often referred to as the tropical tropopause layer (TTL) [Sherwood and Dessler, 2000, 2001]. One main reason is that the detailed mechanism of water vapor dehydration through tropical troposphere-stratosphere exchange is still not clear. While the “freeze and dry” concept [Brewer, 1949] has been generally accepted, the actual freezing mechanism is still controversial. It has been explained as large-scale rising and cooling [e.g., Jensen *et al.*, 2001; Jensen and Pfister, 2004], lifting and cooling by buoyancy disturbances caused by deep convection [e.g., Potter and Holton, 1995; Garrett *et al.*, 2004, 2006], or the adiabatic cooling of air inside deep convection overshooting the level of neutral buoyancy [e.g., Danielsen, 1982; Sherwood and Dessler, 2000]. There are three main keys to distinguish which is the most important process: TTL water vapor, TTL clouds, and deep convection in the vicinity of the TTL.

[3] Measuring TTL water vapor has been challenging. Traditional radiosondes do not provide reliable water vapor measurements at cold temperatures [Elliot and Gaffen, 1991]. Instruments onboard aircraft provide accurate measurements but only during field campaigns. The difficulty in retrieving TTL water vapor from satellite measurements is that water vapor in the TTL exerts little discernible influence on outgoing radiances compared to water vapor at lower heights. Even though there are TTL water vapor retrievals from satellite retrievals on a global scale, low vertical resolution and cloud contamination limit their applicability in the TTL.

[4] The ice clouds in the TTL are radiatively important [e.g., Sassen *et al.*, 1989; Jensen *et al.*, 1996; McFarquhar *et al.*, 2000; Hartmann *et al.*, 2001]. Thus there have been many efforts to measure them using different techniques: by using limb view satellite instruments [e.g., Wang *et al.*, 1996; Massie *et al.*, 2002; Wu *et al.*, 2005], aircraft [McFarquhar *et al.*, 2000], and spaceborne lidar [Dessler *et al.*, 2006].

[5] Before the launch of Tropical Rainfall Measuring Mission (TRMM) [Kummerow *et al.*, 1998], most of the studies describing tropical deep convection in the TTL mainly used IR data [e.g., Gettelman *et al.*, 2002; Massie *et al.*, 2002]. However, it is known that IR measurements

<sup>1</sup>Department of Meteorology, University of Utah, Salt Lake City, Utah, USA.

tend to underestimate cloud height [Sherwood *et al.*, 2004]. Using reflectivity data from the precipitation radar (PR) onboard TRMM, it is possible to infer the intensity of deep convection and its penetration into the TTL quantitatively [Alcala and Dessler, 2002; Liu and Zipser, 2005]. Recently, Liu *et al.* [2006] suggested that there are big differences between the distribution of tropical deep convection viewed by radar and by infrared radiometer.

[6] The motivations for this study include the following:

[7] 1. With precise description of tropical deep convection from TRMM measurements, can we depict the relation of deep convection activity in the TTL and the TTL thin clouds more quantitatively?

[8] 2. With more and longer-period observations from limb scanning satellite instruments, it may now be timely to verify the TTL thin cloud climatology using well developed algorithms.

[9] 3. Recent spaceborne lidar provides accurate TTL thin clouds measurements in two dimensions, providing a unique opportunity to analyze the entire cloud feature. What is the relation between the TTL thin cloud and deep convection from a cloud system point of view?

[10] 4. There has been no paper comparing the seasonal variations of tropical deep convection, TTL thin clouds and water vapor. Liu and Zipser [2005] pointed out that there is a semiannual cycle of deep convection penetrating the TTL viewed from the TRMM PR. Can we relate that to the seasonal variation of TTL clouds, and of water vapor?

[11] In this work, we address these questions by combining the climatology of deep convection, thin clouds, and water vapor in the vicinity of TTL from four independent types of satellite measurements. Section 2 describes the data and analysis methods. Section 3 shows the results. Discussion and comparison with previous work are presented in section 4.

## 2. Data and Methods

### 2.1. Deep Convection Analysis From TRMM

[12] To identify the tropical deep convection in the TTL, 6 years of TRMM PR and visible and infrared scanner (VIIRS) data are matched and grouped into cold cloud features (CCFs) by pixels with the VIIRS 10.8  $\mu\text{m}$  wavelength brightness temperature ( $T_{B11}$ )  $< 210$  K. Then the CCFs' characteristics, such as area of  $T_{B11} < 210$  K and 20 dBZ PR reflectivity at 14 km, are summarized. Liu *et al.* [2006] described this method and demonstrated that there are large regional differences of tropical deep convection viewed from infrared radiometer and radar. In this study, the area of  $T_{B11} < 210$  K in CCFs is used to indicate the area of deep convection reaching the TTL. The mean height of the 210 K level between  $10^{\circ}\text{S}$ – $10^{\circ}\text{N}$  is  $13.6 \text{ km} \pm 1$  standard deviation of 0.14 km according to the  $2.5^{\circ}$  resolution NCEP reanalysis [Kistler *et al.*, 2001]. The area of PR 20 dBZ reaching 14 km inside CCFs is used to indicate strong penetration into the TTL by tropical deep convection [Liu and Zipser, 2005].

### 2.2. Thin Clouds From SAGE II

[13] Limb scanning instruments represented by the Stratospheric Aerosol and Gas Experiment (SAGE) II and Halogen Occultation Experiment (HALOE) are sensitive to the ultra thin subvisual clouds in the TTL [Kent *et al.*, 1993;

Hervig and McHugh, 1999]. Therefore these measurements have been used to demonstrate the climatology of clouds in the TTL [e.g., Wang *et al.*, 1996; Massie *et al.*, 2002]. By using an algorithm similar to the SAGE II cloud detecting algorithm developed by Kent *et al.* [1993], which infers the presence of cloud when the  $1.02 \mu\text{m}$  extinction coefficient is greater than  $0.001 \text{ km}^{-1}$  and the ratio of  $0.525 \mu\text{m}$  extinction coefficient to the  $1.02 \mu\text{m}$  extinction coefficient is greater than 0.95, the subvisual clouds at TTL are identified from version 6.2 SAGE II data during 1985–2004, excluding the years (1991–1995) with contamination by volcanic aerosols [McCormick *et al.*, 1995]. Cloud occurrences at two layers (14–16 km and 16–18 km) inside  $10^{\circ} \times 10^{\circ}$  boxes and in  $10^{\circ}\text{N}$ – $10^{\circ}\text{S}$  each month are calculated as the percentage of events with clouds identified inside each layer.

### 2.3. IWC, Water Vapor, and CO From MLS

[14] Another limb scanning instrument useful for studying the TTL clouds and their relation to water vapor is the Microwave Limb Sounder (MLS). The first MLS was launched on 12 September 1991 onboard the Upper Atmosphere Research Satellite (UARS). Using the UARS MLS, SAGE II and HALOE, Mote *et al.* [1996] found that there was a gradual upward progression of the annual cycle of water vapor into the stratosphere. Methods to retrieve ice water content (IWC) in the TTL from UARS MLS measurements are described by Wu and Jiang [2004], Livesey *et al.* [2005], and Wu *et al.* [2006]. Wu *et al.* [2005] applied the method to UARS MLS data and discussed the relation of TTL IWC to deep convection. The Earth Observing System (EOS) MLS on the AURA mission was launched on 15 July 2004. Besides the water vapor [Livesey *et al.*, 2005, 2006] and IWC retrievals, the EOS MLS data set includes CO retrievals [Livesey *et al.*, 2006]. CO has about a 2 month photochemical life time in the troposphere and could be used as a tracer for the vertical and horizontal transport into the TTL [e.g., Kar *et al.*, 2004]. Thus its difference at different elevations may be used as a good indicator of the intensity of vertical mixing and transport. Our main concerns in using this data set are its coarse vertical resolution:  $\sim 3$  km for water vapor and IWC,  $\sim 4.5$  km for CO, and a wide horizontal field of view ( $167 \text{ km} \times 7 \text{ km}$ ). The observed mean values in such a large sample volume are not comparable to the in situ measurements. For example, there are  $\sim 28\%$  dry biases at 100 hPa when comparing to aircraft water vapor observations [Livesey *et al.*, 2005]. However, this data set still provides the representative water vapor and CO global distributions and seasonal variations. In this work, we compare one full year (2005) of version 1.5 MLS retrieved water vapor, IWC and CO at 68, 100, and 146 hPa levels to the deep convection and TTL clouds climatologies from other measurements. The mean height of 68, 100, and 146 hPa between  $10^{\circ}\text{S}$ – $10^{\circ}\text{N}$  are 18.8 km, 16.6 km, and 14.4 km with 1 standard deviation about 0.03 km according to  $2.5^{\circ}$  resolution NCEP reanalysis data. In this work, all MLS data are processed with requirements described by Livesey *et al.* [2005].

### 2.4. Thin Layer Clouds From ICESat/GLAS

[15] Quite different in principle from the limb scanning techniques, nadir viewing spaceborne lidar provides a very accurate measurement of TTL clouds [Winker and Trepte,

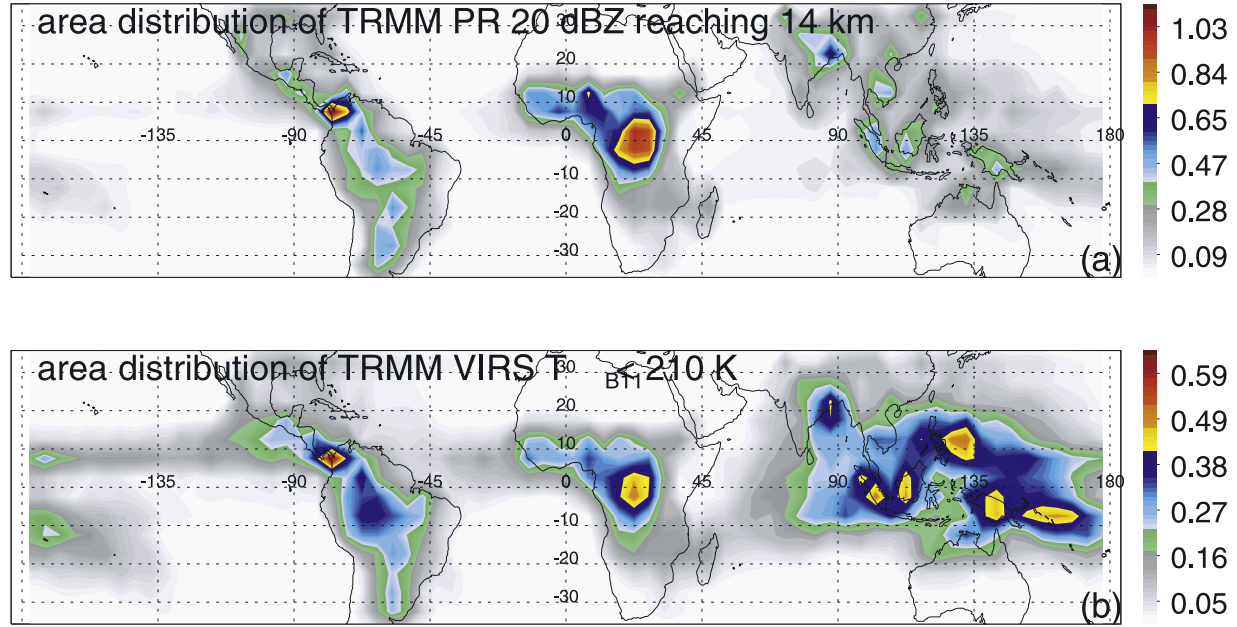


**Figure 1.** (a) Distribution of area of TRMM PR 20 dBZ reaching 14 km in CCFs. The distribution is generated by accumulation of area of PR 20 dBZ reaching 14 km in CCFs in  $5^\circ \times 5^\circ$  boxes from 6 years of TRMM CCFs. The area in each  $5^\circ \times 5^\circ$  box has been divided by the TRMM 3A25 total pixel number to remove the sampling bias. Units are %. (b) Same as Figure 1a but for areas of TRMM VIRS  $T_{B11} < 210$  K.

1998; Hart *et al.*, 2005; Dessler *et al.*, 2006]. The Geoscience Laser Altimeter System (GLAS) onboard the Ice Cloud and Land Elevation Satellite (ICESat) was launched in January 2003. It detects the layer clouds with 76.8 m vertical resolution and optical depth down to 0.01 [Spinhirne *et al.*, 2005]. Dessler *et al.* [2006] analyzed the release 19 GLAS09 products in the TTL on both height and isentropic levels, and reported more TTL thin clouds over land than over ocean, and a weak maximum of cloud occurrence was found in the mid troposphere in isentropic levels. Here we only consider the layer clouds in the release 19 GLAS11 products [Palm *et al.*, 2002] on the height levels and compare the geo distribution and the seasonal variations of these clouds to those from other satellite measurements. 53 days of GLAS11 data from 26 September to 17 November 2003 are analyzed in two steps. First, the layer clouds at the neighboring scans with overlapping cloud top and bottom bracket are grouped into GLAS11 cloud features (GCFs). Then characteristics of each GCF, such as the horizontal size, center location, cloud top, bottom height, mean and max cloud thickness and optical depth are calculated. Because of low horizontal resolution ( $\sim 28$  km), the size of GCFs covering only a few scans could be overestimated. However, the size and properties of large GCFs are relatively reliable and will be shown together with the properties of TRMM CCFs.

### 3. Results

#### 3.1. Geographical Distribution of Deep Convection and Cloud Occurrence From SAGE and MLS IWC

[16] It is known that the regions with TTL thin clouds are climatologically collocated with deep convection identified from IR images [Wang *et al.*, 1996; Dessler and Yang, 2003;

Dessler *et al.*, 2006]. Here results from several different satellite measurements confirm that. Figure 1 shows the tropical deep convection in the vicinity of the TTL for 6 years of CCFs by showing the distribution of areas with  $T_{B11} < 210$  K and 20 dBZ reaching 14 km. The strongest deep convection with 20 dBZ reaching 14 km happens mainly over land (Figure 1a). Liu *et al.* [2006] pointed out that the area covered by these 20 dBZ echoes is only  $\sim 1\%$  of the area of 210 K clouds. There are large areas of deep convection with clouds colder than 210 K and reaching the TTL over west Pacific Ocean without 20 dBZ radar echoes. Using 17 years of SAGE II measurements, the distribution of cloud occurrences in  $10^\circ \times 10^\circ$  boxes at 14–16 km and 16–18 km are generated in Figure 2. Figure 2 shows a similar distribution to that of Wang *et al.* [1996]. SAGE II TTL clouds are detected frequently over the region with deep convection in the TTL as inferred from area of  $T_{B11} < 210$  K. As a comparison, 100 hPa and 146 hPa IWC retrievals from 2005 EOS MLS data set are accumulated in  $10^\circ \times 10^\circ$  boxes and shown in Figure 3. Similar to the comparisons between MLS RHI and SAGE II clouds by Sandor *et al.* [2000], MLS IWC shows a similar geographical distribution as SAGE II cloud occurrence and TTL deep convection in Figure 1b. Total IWC at 100 hPa is about 11% of the total IWC at 146 hPa between  $20^\circ\text{S}$ – $20^\circ\text{N}$ . The number of SAGE II thin clouds at 16–18 km is about 32% of the number of clouds at 14–16 km in  $20^\circ\text{S}$ – $20^\circ\text{N}$ . This may imply that clouds at 16–18 km have relatively less IWC and possibly are optically thinner than the clouds at 14–16 km.

#### 3.2. Geographical Distribution of Thin Clouds From ICESat/GLAS

[17] Using 53 days of GLAS11 data, a total of 185,635 GCFs are defined, where 66,998 of them are between

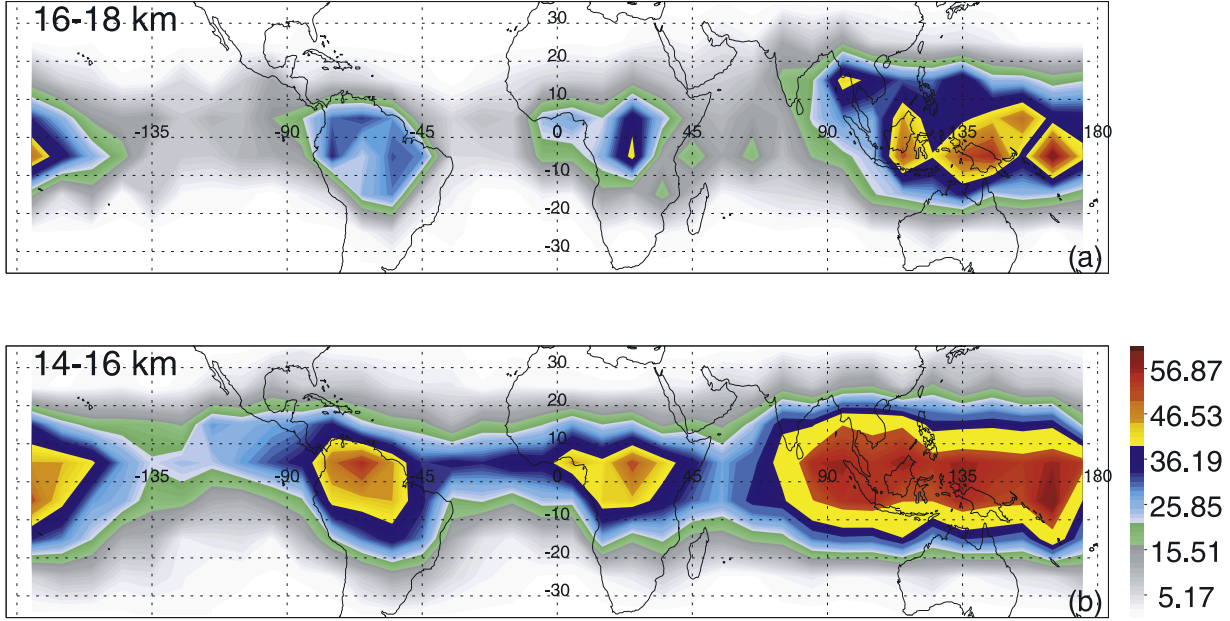


**Figure 2.** (a) Geographical distribution of SAGE II thin cloud occurrence at 16–18 km. Cloud occurrence is obtained from 17 years (1985–1990 and 1996–2004) of SAGE II data. Units are %. (b) Same as Figure 2a but for cloud occurrence at 14–16 km.

35°S–35°N. To demonstrate the TTL cloud geographical distribution, the horizontal coverage of all GCFs with the lowest bottom above 10 and 14 km are accumulated in  $10^\circ \times 10^\circ$  boxes. After normalization with the total coverage, the percentage distribution of GLAS cloud coverage is shown in Figure 4. Most GCFs are found in regions with high-TTL cloud occurrence from SAGE II in Figure 2 and large MLS IWC in Figure 3. However, there are some differences. First, in contrast to the more frequent clouds over the west Pacific Ocean obtained from SAGE II cloud frequency and

MLS IWC, there are more GLAS clouds over the Philippines than over the west Pacific Ocean. This is due to the seasonal change of the cloud frequencies. SAGE II cloud occurrence and MLS IWC in September, October and November (SON) show the same pattern (not shown). Second, GLAS layer clouds above 14 km show a higher relative contribution over central Africa. This is consistent with the high cloud frequency over Africa at the 370 K level reported by *Dessler et al.* [2006]. However, SAGE II suggests higher cloud frequency over the west Pacific.

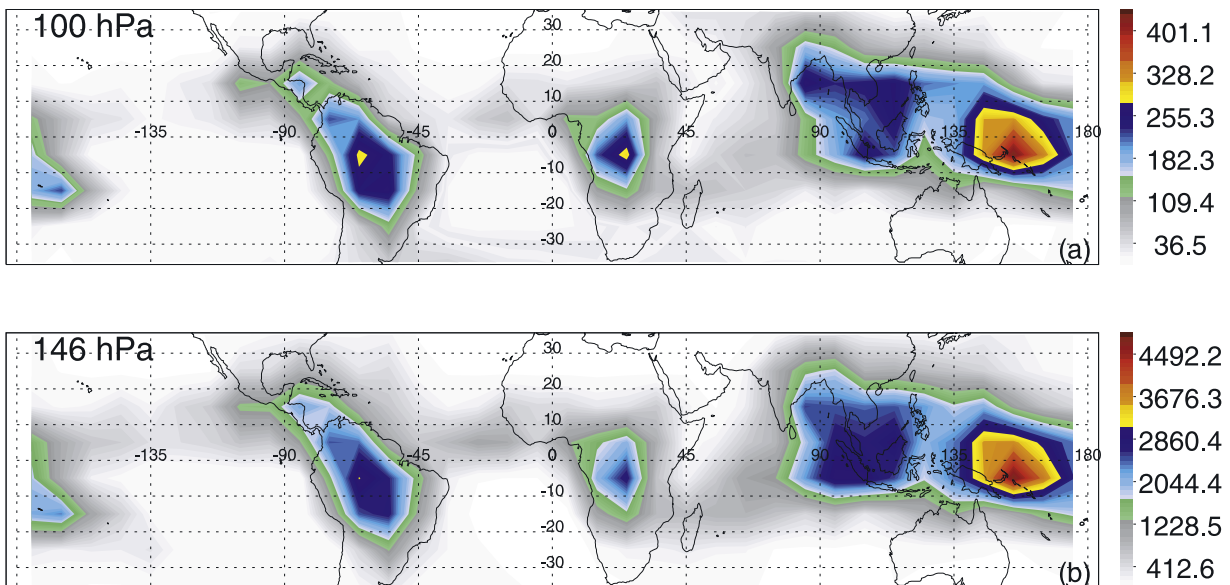


**Figure 3.** (a) Geographical distribution of total accumulation of ice water content in  $10^\circ \times 10^\circ$  boxes at 100 hPa from 2005 AURA MLS data. Units are mg/m<sup>3</sup>. (b) Same as Figure 3a but for 146 hPa.

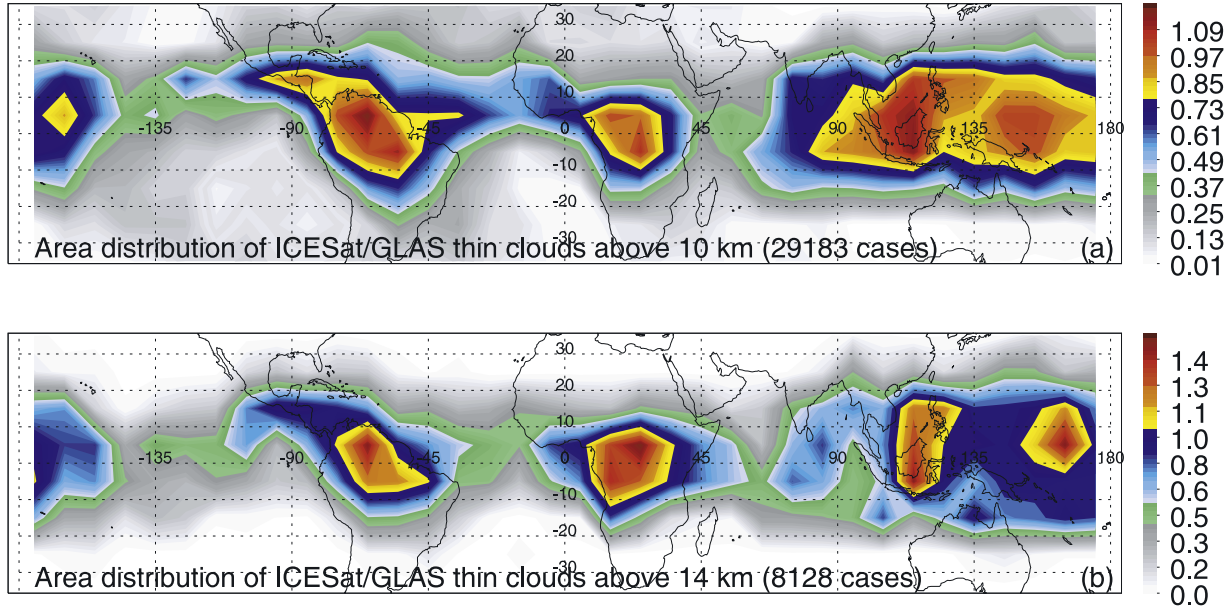


**Figure 4.** (a) Distribution of percent coverage of ICESat/GLAS thin layer clouds above 10 km. The percentages are calculated using two steps: first, accumulating the coverage of GCFs above 10 km in  $10^\circ \times 10^\circ$  boxes, then dividing by total coverage of those GCFs. Units are %. (b) Same as Figure 4a but for the GCFs above 14 km.

The SAGE II instrument has the field of view of 200 km along path, and GLAS has the vertical resolution of 0.076 km. Some large size layer clouds with relatively large optical thickness (e.g., a 100 km wide 1 km thick layer cloud with extinction coefficient of  $0.04 \text{ km}^{-1}$  has optical thickness of 4) may appear opaque in SAGE II data, but are still easily detectable by GLAS.

[18] To relate the TTL GCFs with deep convection CCFs, the GCFs above 14 km are categorized by the rarity of cloud size, thickness and mean optical depth as illustrated in Figure 5. Using a similar procedure, TRMM CCFs in SON 2003 are categorized by the rarity of area of  $T_{B11} < 210 \text{ K}$  and area of 20 dBZ reaching 14 km in Figure 6. Apparently, the location of large and thick TTL GCFs in Figure 5 was close to those very cold CCFs, but not exactly collocated. Since it is possible that thin clouds are the blowoff of deep convection anvils [e.g., *Dessler and Yang, 2003*], the distribution of large (width  $> 100 \text{ km}$ ) and thick (depth  $> 1 \text{ km}$ ) GCFs are shown with area of 210 K CCFs and 20 dBZ at 14 km as well as the 100–150 hPa mean flow calculated from both the ERA40 [*Uppala et al., 2005*] and NCEP reanalyses [*Kistler et al., 2001*] in Figure 7. It is interesting to find that there is a general spatial correlation between the largest, most of the thickest and GCFs and the area with CCFs having the largest area of 210 K over Africa, Amazon and West Pacific. It seems that most GCFs are located downstream of regions with deep convection in the TTL. It may be significant that during SON Argentina and Brazil have the most intense storms [*Zipser et al., 2006*] reaching very high altitudes. However, no layer clouds are found. We speculated that the explanation may be a hostile dry and turbulent environment at 14 km at those latitudes, which could evaporate anvil cirrus relatively quickly. Also,

low relative humidity in this region could limit generation of thin cirrus from gravity waves.

### 3.3. MLS CO and Water Vapor

[19] Since deep convection and TTL clouds are proposed to be playing an important role in the TTL water vapor budget, we now show  $10^\circ \times 10^\circ$  mean MLS water vapor geographical distribution from 2005 MLS data, in spite of large uncertainties of the MLS retrievals. At 146 hPa (Figure 8b), high water vapor mixing ratios are observed in deep convection active regions. However, at 100 hPa (Figure 8a), water vapor mixing ratios are lower in the equatorial region, and are lowest of all over the west Pacific.

[20] Because CO has  $\sim 2$  month lifetime in the troposphere and stratosphere, the amount of TTL CO at upper levels is mainly controlled by vertical transport from the sources at lower levels.  $10^\circ \times 10^\circ$  mean MLS CO mixing ratio in Figure 9 shows the signatures of strong vertical transport by deep convection over Africa, the Amazon, and the high-CO source over India. We suggest that the large CO mixing ratio over Africa is due to vertical transport by strong deep convection from the large surface source of biomass burning.

### 3.4. Seasonal Distribution of Deep Convection, Thin Clouds, and Water Vapor

[21] To understand the relationships among tropical deep convection, TTL clouds and water vapor, it is important to compare their seasonal variations. Figure 10 summarizes  $10^\circ\text{N}-10^\circ\text{S}$  monthly variations of deep convection reaching the TTL indicated from area of TRMM  $T_{B11} < 210 \text{ K}$  and 20 dBZ reflectivity reaching 14 km (Figure 10a), TTL cloud occurrence from SAGE II (Figure 10b), MLS IWC (Figure 10c), water vapor (Figure 10d) and CO (Figure 10e).

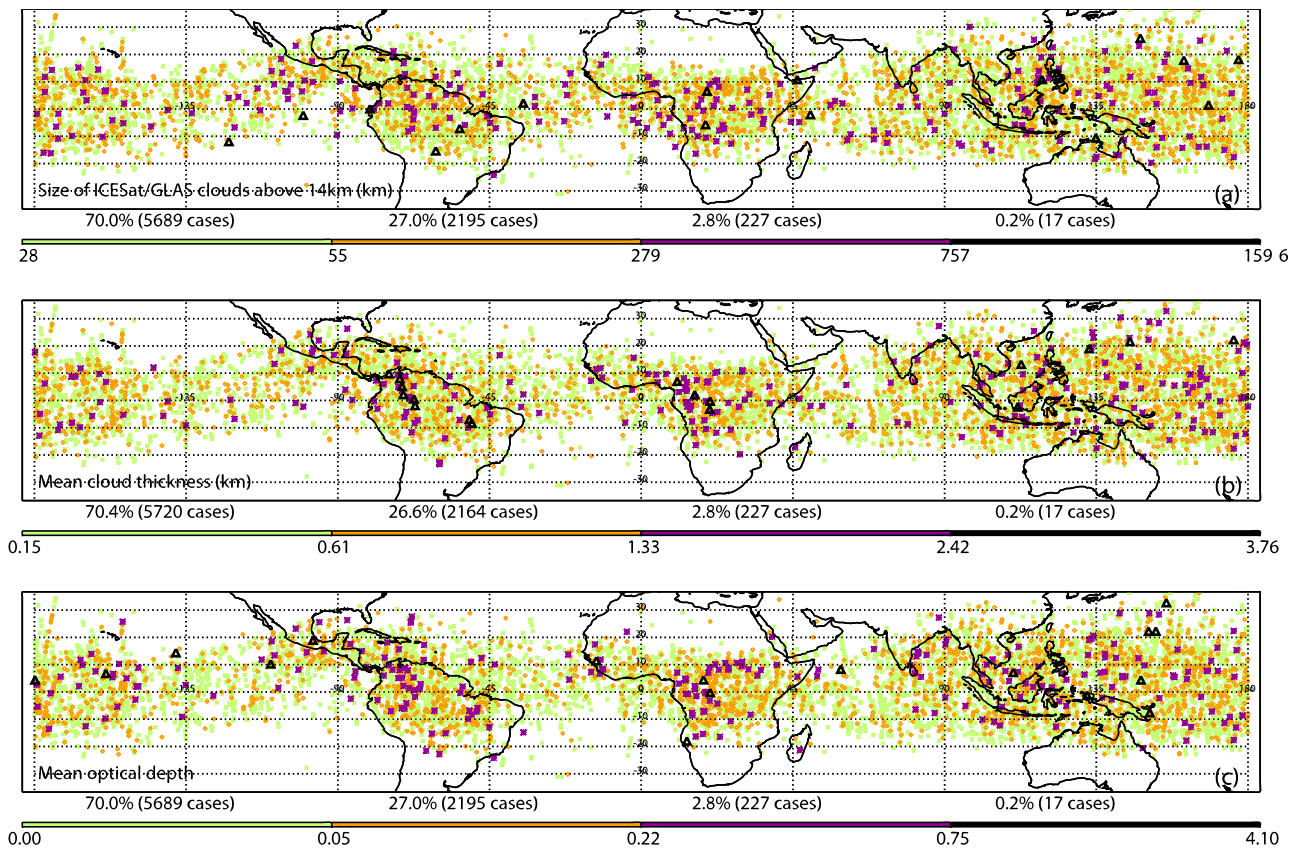


**Figure 5.** Locations of GCFs above 14 km categorized by (a) size, (b) mean thickness, and (c) mean optical depth. Rarity of the events is represented by green dots (approximately bottom 80%), orange diamonds (approximately top 20%), purple asterisks (approximately top 2%), and black triangles (approximately top 0.2%).

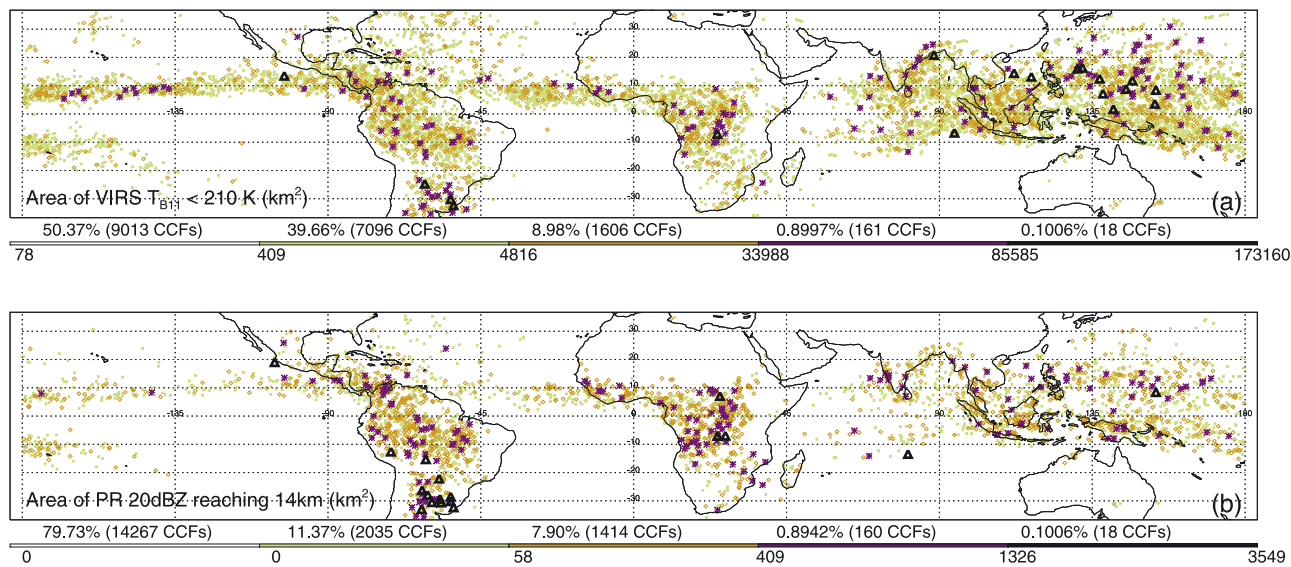


**Figure 6.** Location of September–November 2003 TRMM CCFs ( $\leq 210$  K) categorized by (a) size of  $TB \leq 210$  K and (b) size of 20 dBZ reaching 14 km. Rarity of the events is represented with green dots (approximately top 10%), orange diamonds (approximately top 1%), purple asterisks (approximately top 0.1%), and black triangles (approximately top 0.01%).

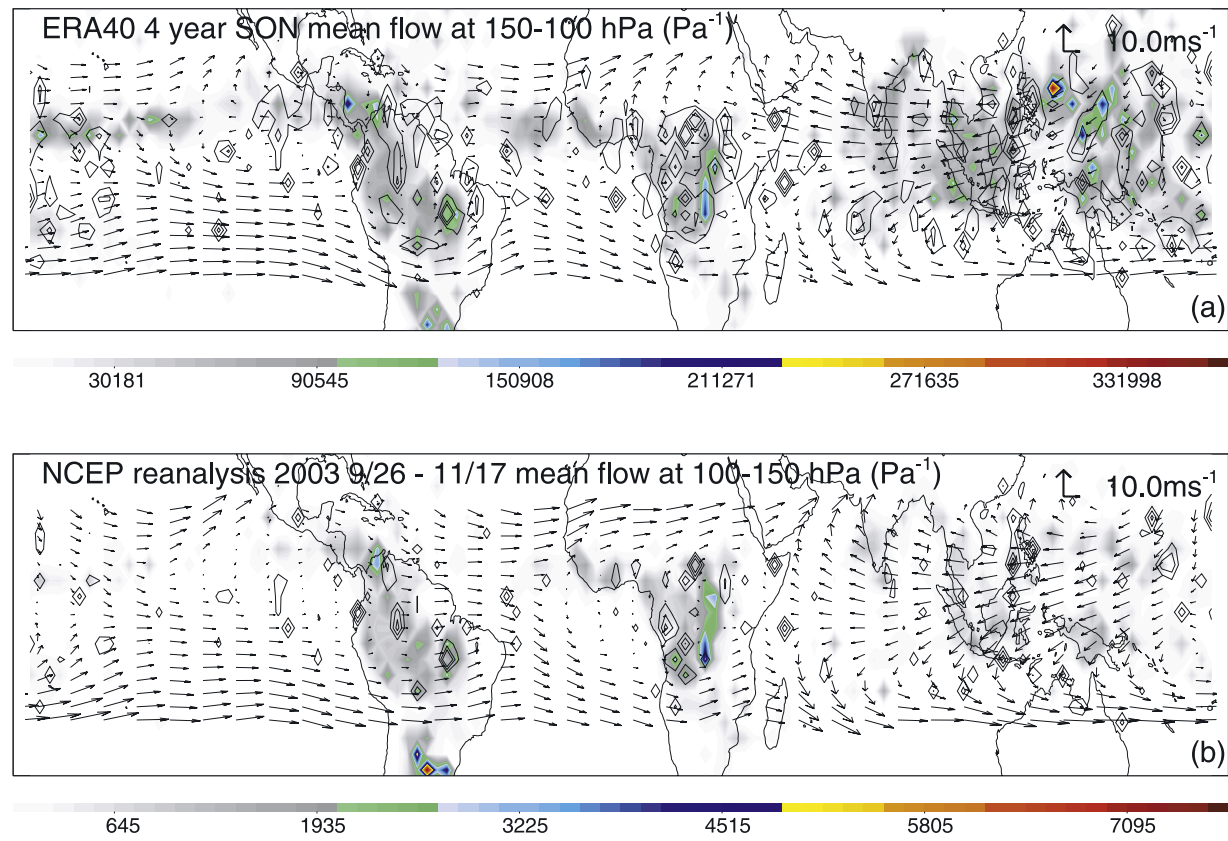


**Figure 7.** (a) Accumulative TRMM VIRS area of  $T_{B11} < 210 \text{ K}$  in  $3^\circ \times 3^\circ$  boxes (color fill) and total coverage of GCFs above 14 km with size above 100 km in the same box (contoured with 300, 600, and 900 km). ERA40 4 year (1998–2001) September, October, and November mean flow between 100 and 150 hPa are overlapped. (b) Accumulative area of TRMM PR 20 dBZ reaching 14 km in  $3^\circ \times 3^\circ$  boxes (color fill) and total coverage of GCFs thicker than 1 km above 14 km in the same box (contoured with 300, 600, and 900 km). NCEP reanalysis 26 September to 17 November mean flow between 100 and 150 hPa are overlapped.

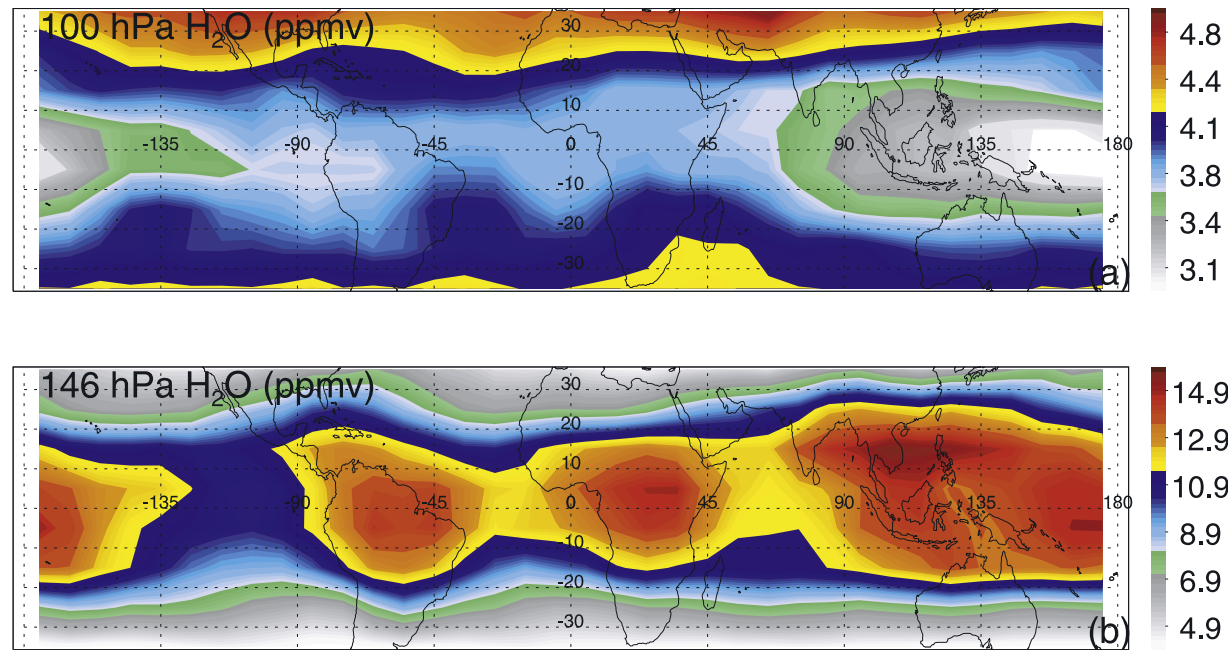


**Figure 8.** The  $10^\circ \times 10^\circ$  mean H<sub>2</sub>O mixing ratio (ppmv) from 2005 version 1.5 EOS MLS data at (a) 100 hPa and (b) 146 hPa.

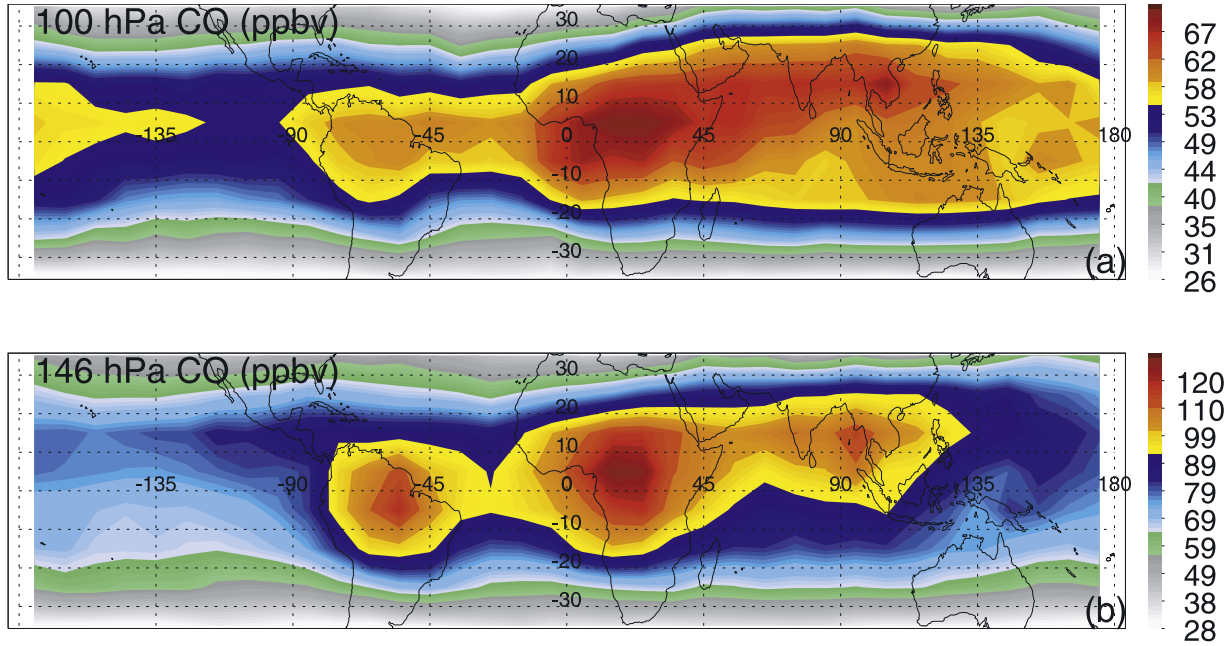


**Figure 9.** The  $10^\circ \times 10^\circ$  mean CO mixing ratio (ppbv) from version 1.5 2005 EOS MLS data at (a) 100 hPa and (b) 146 hPa.

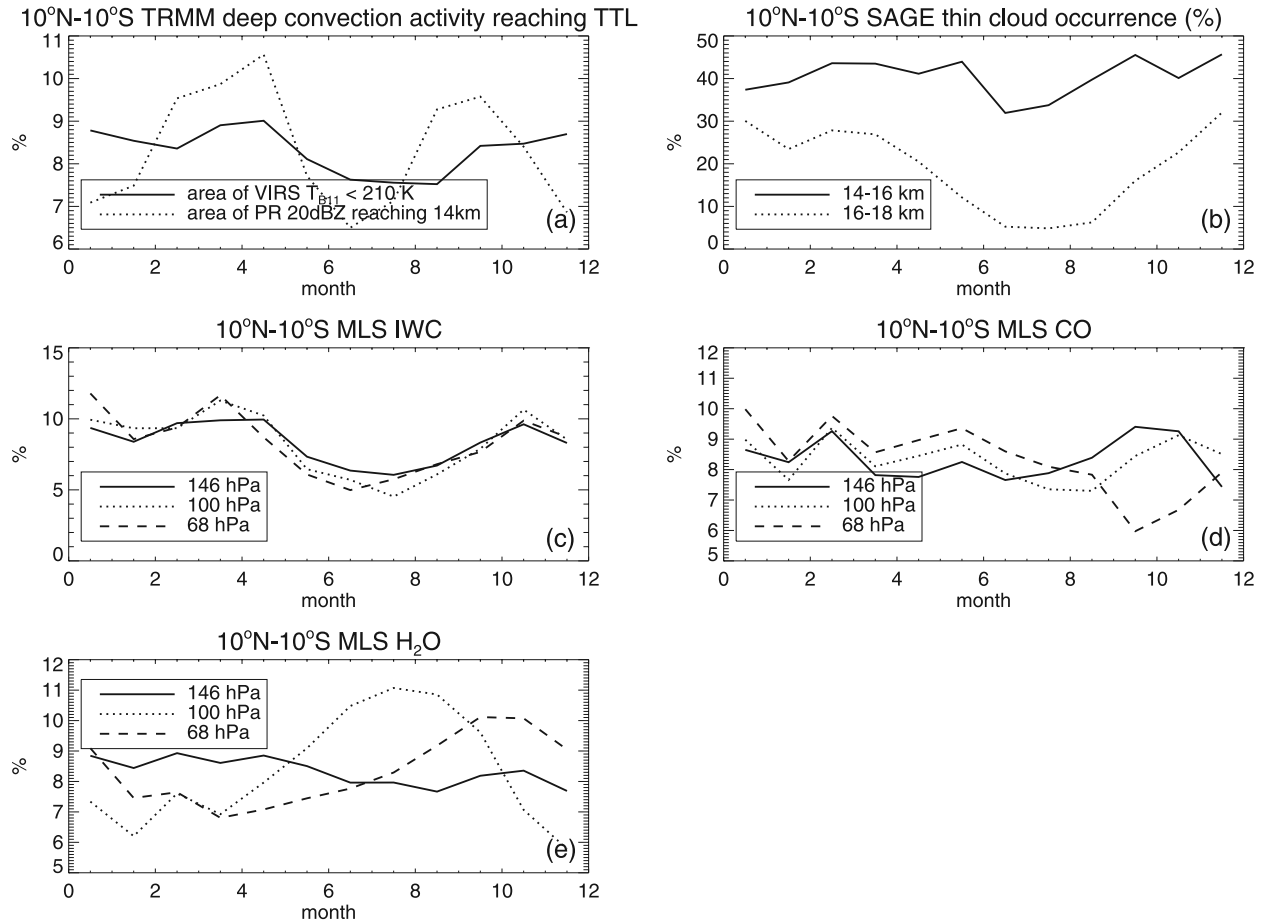


**Figure 10.** Seasonal variation of deep convection, thin clouds, and trace gases in the TTL. (a) Monthly percentage of area of  $T_{B11} < 210\text{ K}$  and 20 dBZ reaching 14 km in TRMM CCFs. (b) Monthly SAGE II thin cloud occurrence at 14–16 km and 16–18 km. (c) Monthly percentage of accumulated MLS IWC. (d) Monthly percentage of total MLS CO. (e) Monthly percentage of total MLS H<sub>2</sub>O.

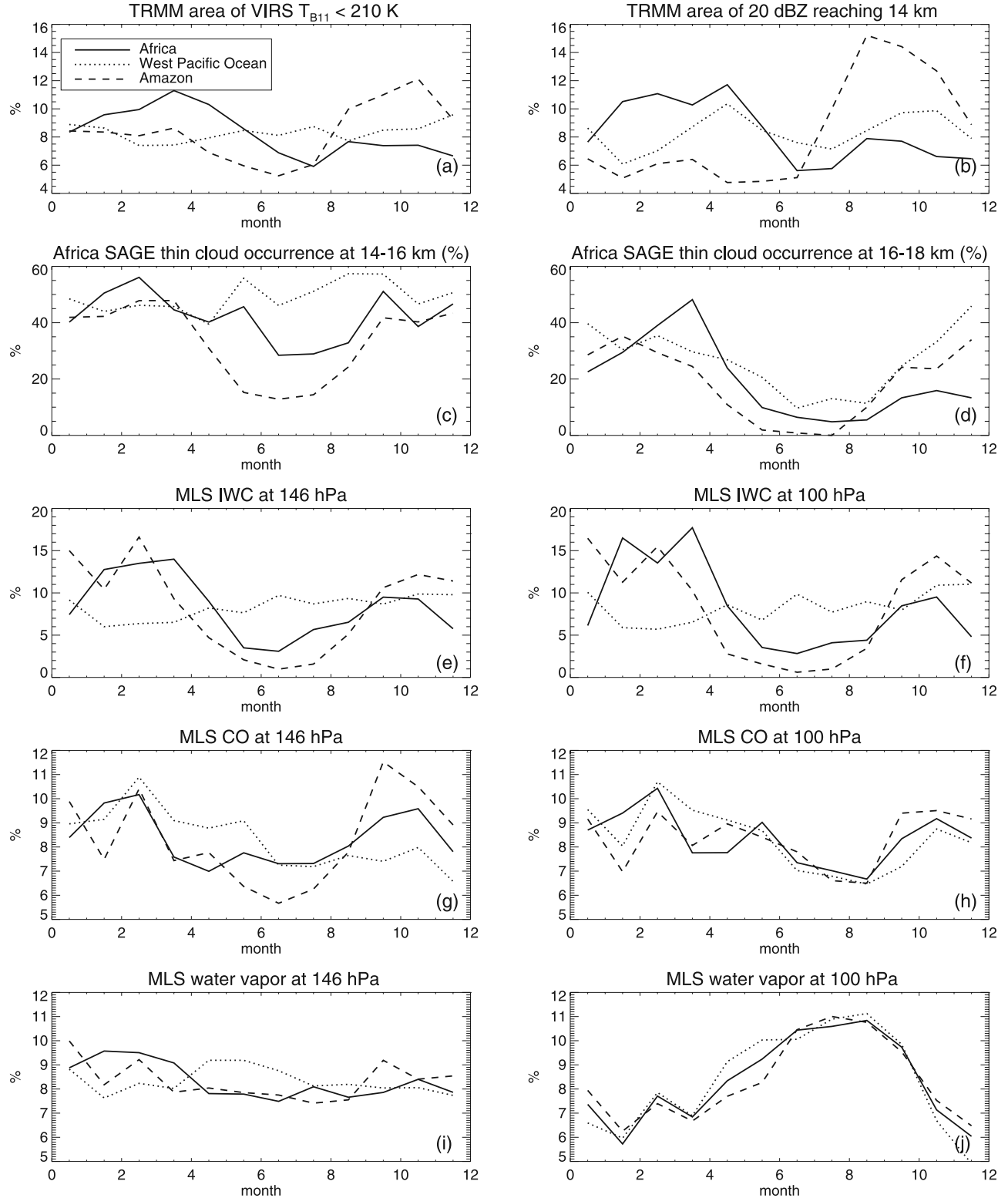


**Figure 11.** Similar to Figure 10 but comparing the results from samples over central Africa ( $10^{\circ}\text{S}$ – $10^{\circ}\text{N}$ ,  $0$ – $45^{\circ}\text{E}$ ), west Pacific Ocean ( $10^{\circ}\text{S}$ – $20^{\circ}\text{N}$ ,  $90$ – $180^{\circ}\text{E}$ ), and Amazon ( $0^{\circ}$ – $20^{\circ}\text{S}$ ,  $45$ – $90^{\circ}\text{W}$ ) at 146 hPa and 100 hPa.

As pointed out by Liu and Zipser [2005], there is a semiannual cycle of tropical deep convection based upon the 20 dBZ echoes reaching the TTL. However, the area of 210 K clouds shows an annual cycle (Figure 10a), and has a

similar pattern to the seasonal cycles of SAGE II thin cloud occurrence, MLS IWC, 146 hPa water vapor and CO. There is a negative correlation between the seasonal cycles of the TTL clouds and MLS 100 hPa water vapor.

[22] To demonstrate the regional variation of the seasonal cycle, the monthly variations of deep convection, TTL cloud and water vapor measurements have been analyzed over Africa, Amazon and the west Pacific Ocean in Figure 11. It is obvious that deep convection reaching the TTL inferred from 210 K cloud area over Africa has a different monthly variation pattern from that over the west Pacific Ocean. A semiannual cycle of 20 dBZ reaching 14 km over west Pacific is most likely due to coastal effects from a few (Figure 1a) deep convection systems over adjacent land. The patterns of regional differences of deep convection seasonal cycles are also found in regional differences of seasonal cycles of SAGE II thin clouds, MLS IWC, and 146 hPa MLS CO and water vapor. However, there is almost no regional variation of seasonal cycles of MLS CO and water vapor at 100 hPa. This can be explained with the well mixed air at those levels on monthly timescales. Similar to the results of Schoeberl *et al.* [2006], in Figures 10 and 11 MLS CO seasonal variation at 100 hPa and 68 hPa is negatively correlated with water vapor.

## 4. Discussion

### 4.1. Relation Between Deep Convection and TTL Thin Clouds

[23] Data from independent satellite instruments demonstrate that tropical deep convection in the TTL derived from area of 210 K clouds has a good correlation with TTL thin clouds both geographically and seasonally. Large, thick TTL clouds observed by lidar are found downstream of the active deep convection regions. These all suggest that TTL thin clouds are strongly related to tropical deep convection. However, whether TTL thin clouds are generated by the detrainment from deep convection turrets penetrating the TTL, blow off of anvil clouds, or buoyancy disturbances by deep convection is still a mystery and beyond the scope of this study.

[24] A semiannual cycle of area of 20 dBZ reaching 14 km, characteristic of intense deep convection, is found in many different regions. However, the area of  $T_{B11} < 210$  K is better correlated with TTL cloud geographically and seasonally. This suggests that relatively weaker deep convection without precipitation ice particles lifted to 14 km shown as high reflectivity by PR (e.g., deep convection over the west Pacific Ocean) also plays an important role in TTL cloud statistics. However, more layer clouds found over Africa by lidar than by SAGE II imply that there might be regional differences of TTL cloud properties. This could be related to the regional difference of intensities of deep convection and needs further investigation.

[25] On the basis of the above results from deep convection, TTL clouds and EOS MLS measurements, we hypothesize that deep convection reaching the TTL introduces saturated air into the lower TTL at 14–15 km. Large-scale rising and cooling of this air may cause supersaturation with respect to ice ( $RHI > 1.0$ ). After ice particles in TTL clouds are introduced in the lower TTL by deep convection (by a still-unclear mechanism), deposition process under  $RHI > 1.0$  environment would dehydrate air further. It is not likely that most of the TTL clouds live long enough to travel long distances, because if that were true, high cloud frequency would be the greatest well downstream from where they are

generated. Also the regional differences would not exist in the seasonal cycle of TTL clouds as observed.

### 4.2. Reviews of the Hypothesis of Dehydration in the TTL

[26] There were some model studies [e.g., Jensen and Pfister, 2004, 2005] suggesting that the TTL cloud distribution and dehydration may be simulated by ice particles generated by slow large-scale rising. However, these simulations do not include the impact of deep convection. Without considering the relatively larger ice particles in the TTL introduced by deep convection, the model simulation ice particles have smaller size, and thus would live longer in the TTL. As a result, in the simulations, some of clouds may live several days and drift downstream for a large distance. Results of regional difference of the TTL cloud seasonal cycle here implies that even if the thin clouds were generated, they do not live long enough to deposit more water vapor and cause further dehydration. Further, with no deep convection influence, simulations seem to underestimate the cloud amount over land.

[27] Holton and Gettelman [2001] have suggested a dehydration process due to horizontal transport through the coldest tropopause over the west Pacific during Northern Hemisphere winter. If that were the case, then more TTL clouds in the inflow region of cold tropopause over the west Pacific Ocean would be observed. However, more large and thick GCFs were found downstream of the flow. Because the GLAS data used here do not extend to the winter time, this contradiction is not conclusive and needs more observations for verification.

[28] If we assume that the strongest overshooting can be represented by the area of 20 dBZ reaching 14 km, then the direct dehydration by the cold air overshooting the LNB may be used to explain the TTL cloud and dehydration over Africa, Panama and Indonesia. However, this cannot explain the TTL clouds over West Pacific Ocean. One possibility for these thin cirrus clouds is through the buoyancy disturbance suggested by Potter and Holton [1995] and Garrett *et al.* [2004]. Convection over the west Pacific Ocean does not have strong enough updrafts to lift precipitation size particles to high altitudes and penetrate deep into the TTL. However, the gravity waves from it may generate thin clouds given a humid environment [Newell *et al.*, 1996; Luo *et al.*, 2007]. The negative correlation between seasonal variation of TTL CO and water vapor suggests that there is a good correlation between dehydration in the TTL and the convective transport.

### 4.3. Future Work

[29] On the basis of these results and discussion, some interesting topics are worthy of investigation in the future:

[30] 1. The description of deep convection by cold cloud area and 20 dBZ radar echo reaching high altitude from TRMM PR do not give enough information to understand the weak convection over the west Pacific. CloudSat and CALIPSO were launched in April 2006. They are providing detailed information of thin TTL clouds and the top part of clouds from weak convection over the West Pacific Ocean. Searching the layer clouds above the convective clouds from these data would be a key to test the hypothesis of dehydration by buoyancy disturbance.

[31] 2. Some large size TTL clouds are found by GLAS downstream of areas with strong deep convection reaching the TTL. However, there is little direct evidence to relate these TTL clouds to individual deep convection systems. Therefore, to understand the evolution and longevity of TTL clouds from deep convection, case studies of GCFs and their time evolution are needed. Also, it is important to make use of the intensive observations in field campaigns such as the Tropical Warm Pool International Cloud Experiment (TWP-ICE), which could provide detailed information on the mechanism of the generation of TTL clouds related to deep convection.

[32] 3. Because TTL thin clouds are closely related to deep convection, there must be an impact of the strong diurnal cycle of deep convection on the diurnal variations of TTL clouds. Also, diurnal variation of TTL clouds would have a large impact on the radiation budget. However, all of the current measurements of thin clouds and water vapor are from instruments onboard sun synchronous satellites. Even with this limitation, study of diurnal changes of TTL clouds at 2 times/day may still provide useful hints.

## 5. Summary

[33] Geographical and seasonal distributions of deep convection and clouds in the vicinity of the TTL using data from independent spaceborne instruments (TRMM PR and VIRS, SAGE II, ICESat/GLAS MLS) are compared. Thin clouds in the TTL inferred from SAGE II cloud occurrence and MLS IWC are more frequently observed near the regions with deep convection in the TTL inferred from area of TRMM VIRS  $T_{B11} < 210$  K: the west Pacific, central Africa, Panama, and the Amazon. There are good correlations among seasonal cycles of area of 210 K clouds, TTL SAGE II cloud occurrence, and MLS IWC. The patterns of regional differences of deep convection seasonal cycles are found in the seasonal cycles of TTL clouds as well. The largest, thickest, TTL clouds with the highest optical depth from lidar observations are found seemingly downstream of regions with deep convection reaching the TTL. All these suggest that TTL thin clouds are closely coupled with deep convection reaching into the TTL. MLS water vapor at 100 hPa shows a negative correlation with TTL clouds geographically and seasonally. MLS CO is positively correlated with deep convection at 147 hPa geographically and seasonally. However, it is negatively correlated with water vapor at 100 hPa.

[34] **Acknowledgments.** Thanks are due the SAGE II group, EOS MLS group, and ICESat/GLAS group for their hard work in creating the extraordinary data sets. MLS water vapor and CO data were downloaded from NASA DAAC/GSFC. MLS IWC data are provided by Jonathan Jiang. All MLS data are processed following recommendations from Livesey *et al.* [2005]. GLAS data were downloaded from National Snow and Ice Data Center (NSIDC). Thanks to Ed Zipser for his suggestions and English revision. Useful comments from Jonathon Jiang, Andrew Dessler, Steve Sherwood, and Tim Garrett and two anonymous reviewers are gratefully acknowledged. This work was supported by the NASA TRMM office under grant NAG5-13628. The TRMM data were processed by the TRMM Science Data and Information System (TSDIS).

## References

- Alcala, C. M., and A. E. Dessler (2002), Observations of deep convection in the tropics using the Tropical Rainfall Measuring Mission (TRMM) precipitation radar, *J. Geophys. Res.*, 107(D24), 4792, doi:10.1029/2002JD002457.
- Brewer, A. M. (1949), Evidence for a world circulation provided by the measurements of helium and water vapor distribution in the stratosphere, *Q. J. R. Meteorol. Soc.*, 75, 351–363.
- Danielsen, E. F. (1982), A dehydration mechanism for the stratosphere, *Geophys. Res. Lett.*, 9, 605–608.
- Dessler, A. E., and P. Yang (2003), The distribution of tropical thin cirrus clouds inferred from Terra MODIS data, *J. Clim.*, 16, 1241–1248.
- Dessler, A. E., S. P. Palm, and J. D. Spinhirne (2006), Tropical cloud-top height distributions revealed by the Ice, Cloud, and Land Elevation Satellite (ICESat)/Geoscience Laser Altimeter System (GLAS), *J. Geophys. Res.*, 111, D12215, doi:10.1029/2005JD006705.
- Elliot, W. P., and D. J. Gaffen (1991), On the utility of radiosonde humidity archives for climate studies, *Bull. Am. Meteorol. Soc.*, 72, 1507–1520.
- Garrett, T. J., A. J. Heymsfield, M. J. McGill, B. A. Ridley, D. G. Baumgardner, T. P. Bui, and C. R. Webster (2004), Convective generation of cirrus near the tropopause, *J. Geophys. Res.*, 109, D21203, doi:10.1029/2004JD004952.
- Garrett, T. J., Dean-Day, C. Liu, B. K. Barnett, G. G. Mace, D. G. Baumgardner, C. R. Webster, T. Paul Bui, W. R. Read, and P. Minnis (2006), Convective formation of pileus cloud near the tropopause, *Atmos. Chem. Phys.*, 6, 1185–1200.
- Gettelman, A., M. L. Salby, and F. Sassi (2002), Distribution and influence of convection in the tropical tropopause region, *J. Geophys. Res.*, 107(D10), 4080, doi:10.1029/2001JD001048.
- Hart, W. D., J. D. Spinhirne, S. P. Palm, and D. L. Hlavka (2005), Height distribution between cloud and aerosol layers from the GLAS spaceborne lidar in the Indian Ocean region, *Geophys. Res. Lett.*, 32, L22S06, doi:10.1029/2005GL023671.
- Hartmann, D. L., J. R. Holton, and Q. Fu (2001), The heat balance of the tropical tropopause, cirrus, and stratospheric dehydration, *Geophys. Res. Lett.*, 28, 1969–1972.
- Hervig, M., and M. McHugh (1999), Cirrus detection using HALOE measurements, *Geophys. Res. Lett.*, 26, 719–722.
- Holton, J. R., and A. Gettelman (2001), Horizontal transport and the dehydration of the stratosphere, *Geophys. Res. Lett.*, 28, 2799–2802.
- Jensen, E., and L. Pfister (2004), Transport and freeze-drying in the tropical tropopause layer, *J. Geophys. Res.*, 109, D02207, doi:10.1029/2003JD004022.
- Jensen, E., and L. Pfister (2005), Implications of persistent ice supersaturation in cold cirrus for stratospheric water vapor, *Geophys. Res. Lett.*, 32, L01808, doi:10.1029/2004GL021125.
- Jensen, E. J., O. B. Toon, H. B. Selkirk, J. D. Spinhirne, and M. R. Schoeberl (1996), On the formation and persistence of subvisible cirrus clouds near the tropical tropopause, *J. Geophys. Res.*, 101, 21,361–21,375.
- Jensen, E. J., L. Pfister, A. S. Ackerman, A. Tabazadehm, and O. B. Toon (2001), A conceptual model of the dehydration of air due to freeze-drying by optically thin, laminar cirrus rising slowly across the tropical tropopause, *J. Geophys. Res.*, 106, 17,237–17,252.
- Kar, J., et al. (2004), Evidence of vertical transport of carbon monoxide from Measurements of Pollution in the Troposphere (MOPITT), *Geophys. Res. Lett.*, 31, L23105, doi:10.1029/2004GL021128.
- Kent, G. S., D. M. Winker, M. T. Osborn, and K. M. Skeens (1993), A model for the separation of cloud and aerosol in SAGE II occultation data, *J. Geophys. Res.*, 98, 20,725–20,735.
- Kistler, R., et al. (2001), The NCEP-NCAR 50-year reanalysis: Monthly means CD-ROM and documentation, *Bull. Am. Meteorol. Soc.*, 82, 247–267.
- Kummerow, C., and W. Barnes (1998), The tropical rainfall measuring mission (TRMM) sensor package, *J. Atmos. Oceanic Technol.*, 15, 809–817.
- Liu, C., and E. J. Zipser (2005), Global distribution of convection penetrating the tropical tropopause, *J. Geophys. Res.*, 110, D23104, doi:10.1029/2005JD006063.
- Liu, C., E. J. Zipser, and S. W. Nesbitt (2006), Global distribution of tropical deep convection: Different perspectives using infrared and radar as the primary data source, *J. Clim.*, 20, 489–503.
- Livesey, N. J., et al. (2005), Earth Observing Systems (EOS) Microwave Limb Sounder (MLS) version 1.5 level 2 data quality and description document, version 1.51, Jet Propul. Lab., Pasadena, Calif.
- Livesey, N. J., W. V. Snyder, W. G. Read, and P. A. Wagner (2006), Retrieval algorithms for the EOS Microwave Limb Sounder (MLS) instrument, *IEEE Trans. Geosci. Remote Sens.*, 44, 1144–1155.
- Luo, Z., D. Kley, R. H. Johnson, and H. Smit (2007), Ten years of measurements of tropical-tropospheric water vapor by MOZAIC, part I: Climatology, variability, transport and relation to deep convection, *J. Clim.*, 20, 418–435.
- Massie, S., A. Gettelman, W. Randel, and D. Baumgardner (2002), Distribution of tropical cirrus in relation to convection, *J. Geophys. Res.*, 107(D21), 4591, doi:10.1029/2001JD001293.

- McCormick, M. P., L. W. Thomason, and C. R. Trepte (1995), Atmospheric effects of the Mount Pinatubo eruption, *Nature*, **373**, 399–404.
- McFarquhar, G. M., A. J. Heymsfield, J. Spinharne, and B. Hart (2000), Thin and subvisual tropopause tropical cirrus: Observations and radiative impacts, *J. Atmos. Sci.*, **57**, 1841–1853.
- Mote, P. W., K. H. Rosenlof, M. E. McIntyre, E. S. Carr, J. C. Gille, J. R. Holton, J. S. Kinnarsley, H. C. Pumphrey, J. M. Russell III, and J. W. Waters (1996), An atmospheric tape recorder: The imprint of tropical tropopause temperature on stratospheric water vapor, *J. Geophys. Res.*, **101**, 3989–4006.
- Newell, R. E., Y. Zhu, E. V. Browell, W. G. Read, and J. W. Waters (1996), Walker circulation and tropical upper tropospheric water vapor, *J. Geophys. Res.*, **101**, 1961–1974.
- Palm, S., W. Hart, D. Hlavka, E. J. Welton, A. Mahesh, and J. Spinharne (2002), Geosciences Laser Altimeter System (GLAS) atmospheric data products, algorithm theoretical basis document, version 4.2, 137 pp., NASA Goddard Space Flight Cent., Greenbelt, Md.
- Potter, B. E., and J. R. Holton (1995), The role of monsoon convection in the dehydration of the lower tropical stratosphere, *J. Atmos. Sci.*, **52**, 1034–1050.
- Sandor, B. J., E. J. Jensen, E. M. Stone, W. G. Read, J. W. Waters, and J. L. Mergenthaler (2000), Upper tropospheric humidity and thin cirrus, *Geophys. Res. Lett.*, **27**, 2645–2648.
- Sassen, K., M. K. Griffin, and G. C. Dodd (1989), Optical scattering and microphysical properties of subvisible cirrus clouds, and climatic implications, *J. Appl. Meteorol.*, **28**, 91–98.
- Schoeberl, M. R., B. N. Duncan, A. R. Douglass, J. Waters, N. Livesey, W. Read, and M. Filipiak (2006), The carbon monoxide tape recorder, *Geophys. Res. Lett.*, **33**, L12811, doi:10.1029/2006GL026178.
- Sherwood, S. C., and A. E. Dessler (2000), On the control of stratospheric humidity, *Geophys. Res. Lett.*, **27**, 2513–2516.
- Sherwood, S. C., and A. E. Dessler (2001), A model for transport across the tropical tropopause, *J. Atmos. Sci.*, **58**, 765–779.
- Sherwood, S. C., J.-H. Chae, P. Minnis, and M. McGill (2004), Underestimation of deep convective cloud tops by thermal imagery, *Geophys. Res. Lett.*, **31**, L11102, doi:10.1029/2004GL019699.
- Spinharne, J. D., S. P. Palm, W. D. Hart, D. L. Hlavka, and E. J. Welton (2005), Cloud and aerosol measurements from GLAS: Overview and initial results, *Geophys. Res. Lett.*, **32**, L22S03, doi:10.1029/2005GL023507.
- Uppala, S. M., et al. (2005), The ERA-40 re-analysis, *Q. J. R. Meteorol. Soc.*, **131**, 2961–3012.
- Wang, P. H., P. Minnis, M. P. McCormick, G. S. Kent, and K. M. Skeens (1996), A 6-year climatology of cloud occurrence frequency from stratospheric aerosol and gas experiment II observations (1985–1990), *J. Geophys. Res.*, **101**, 29,407–29,429.
- Winker, D. M., and C. R. Trepte (1998), Laminar cirrus observed near the tropical tropopause by LITE, *Geophys. Res. Lett.*, **25**, 3351–3354.
- Wu, D. L., and J. H. Jiang (2004), EOS MLS algorithm theoretical basis for cloud measurements, *JPL Doc. D-19299/CL#04-2160*, Jet Propul. Lab., Pasadena, Calif.
- Wu, D. L., W. G. Read, A. E. Dessler, S. C. Sherwood, and J. H. Jiang (2005), UARS MLS cloud ice measurements and implications for  $H_2O$  transport near the tropopause, *J. Atmos. Sci.*, **62**, 518–530.
- Wu, D. L., J. H. Jiang, and C. P. Davis (2006), EOS MLS cloud ice measurements and cloudy-sky radiative transfer model, *IEEE Trans. Geosci. Remote Sens.*, **44**, 1156–1165.
- Zipser, E. J., D. Cecil, C. Liu, S. W. Nesbitt, and S. Yorty (2006), Where are the most intense thunderstorms on Earth?, *Bull. Am. Meteorol. Soc.*, **87**, 1057–1071.

C. Liu, Department of Meteorology, University of Utah, 135 S 1460 E, Rm. 819, Salt Lake City, UT 84112-0110, USA. (liuct@met.utah.edu)